INTER LIBRARY LOAN REQUEST FORM

Borrower's Name	D. SAUNDERS	Org. or A.U.	1644	Phone	308-3976
Serial Number	337,756	Date of Request	2/7/01	Date Needed By	2/12/01

Please Attach Copy Of Abstract, Citation, Or Bibliography, If Available. Please Provide Complete Citation. Only One Request Per Form.

Author/Editor:	BARDIES et al
Journal/Book Title:	JOUR OF NUCLEAR MEDICINE
Article Title:	BISPECIFIC ANTIBODY ....
Volume (Issue):	37
Pages:	1853 - 1859
Year of Publication:	1996
Publisher:	
Remarks:	

My Pg of Pubs

STIC Use Only RM845.J78 &MIC Accession Number: _____

LIBRARY ACTION	LC		NAL		NIH		NLM		NBS		PTO		OTHER	
	1st	2nd	1st	2nd	1st	2nd	1st	2nd	1st	2nd	1st	2nd	1st	2nd
Local Attempts														
Date														
Initials														
Results														
Examiner Called														
Page Count														
Money Spent														

Provided By: Source and Date

Ordered From: Source and Date

Remarks/Comments

1st & 2nd denotes time taken to a library

O/N - Under NLM means Overnight Service

FX - Means Faxed to us

Bispecific Antibody and Iodine-131-Labeled Bivalent Hapten Dosimetry in Patients with Medullary Thyroid or Small-Cell Lung Cancer

Manuel Bardiès, Stephane Bardet, Alain Faivre-Chauvet, Patrick Peltier, Jean-Yves Douillard, Marc Mahé, Maryse Fiche, Albert Lisbona, Françoise Giacalone, Pascal Meyer, Emmanuel Gautherot, Eric Rouvier, Jacques Barbet and Jean-François Chatal

INSERM Research Unit 211 and Regional Cancer Center, Nantes, France; Immunotech SA, Marseille, France

The purpose of this study was to estimate the dose delivered to tumor targets and normal tissues after two-step injection of an anti-CEA/anti-DTPA-In (F6-734) bispecific antibody and a ^{131}I-labeled di-DTPA In-TL bivalent hapten in patients with medullary thyroid carcinoma (MTC) and small-cell lung cancer (SCLC). **Methods:** Five patients with persistent disease or recurrences of MTC and five patients with primary SCLC or relapse were studied. In a first step, 0.1 to 0.3 mg/kg of F6-734 bispecific antibody was injected intravenously. Four days later, 6 nmole (5.8 to 9.8 mCi) of ^{131}I-labeled di-DTPA In-TL bivalent hapten were injected. Quantitative imaging was performed during one week after the second injection. **Results:** All 5 patients with MTC showed positive immunoscintigraphy (IS). In the smallest visualized and resected tumor (0.8 g), the fraction of injected activity per gram (% ID/g) was 0.1% at Day 3. IS was positive in 4 of the 5 patients with SCLC. The volume of the smallest visualized SCLC tumor was estimated at 11 ± 2 ml, and tumor uptake was about 0.009% ID/g. Tumor dose estimates ranged from 4.2 to 174 cGy/mCi in patients with MTC and from 1.7 to 8 cGy/mCi in patients with SCLC. **Conclusion:** High absorbed dose values were calculated for small MTC recurrences. For SCLC recurrences the values were smaller but in the same range as those obtained by other investigators with the one-step technique in lymphoma.

Key Words: bispecific antibody; two-step targeting; medullary thyroid cancer; small-cell lung cancer

J Nucl Med 1996; 37:1853–1859

Despite the promising results obtained for refractory lymphomas with ^{131}I-labeled monoclonal antibodies (MAbs) (*1,2*), the efficacy of radioimmunotherapy (RIT) with directly labeled antibodies remains limited. Two-step radioimmunotargeting reduces radioactive concentration in normal tissues, thereby increasing tumor-to-normal tissue ratios (*3*). In colorectal carcinoma, tumor-to-blood and tumor-to-liver ratios obtained after two-step injection of nonradiolabeled bispecific anti-carcinoembryonic antigen (CEA)/anti-In-DTPA antibody (BsMAb) and ^{111}In-labeled di-DTPA In-TL bivalent hapten were respectively 1.9- and 3.5-fold higher than those achieved after one-step injection of F(ab')$_2$ fragments of the same ^{111}In-labeled anti-CEA antibody (*4*). Similar results have been obtained in relapses of medullary thyroid cancer (MTC) with the same BsMAb and ^{111}In-labeled bivalent hapten (*5*). These data, extrapolated to ^{131}I, are favorable to RIT application since irradiation of normal tissues with the two-step technique at an equivalent injected activity would be lower than with the one-step technique.

The purpose of this RIT feasibility study in patients with MTC or small-cell lung cancer (SCLC) was to estimate the radiation dose delivered to known tumor targets and normal tissues after two-step injection of a nonradiolabeled anti-CEA/anti-In-DTPA BsMAb and a ^{131}I-labeled di-DTPA In-TL bivalent hapten.

Received Sept. 11, 1995; revision accepted Jan. 28, 1996.

For correspondence or reprints contact: Jean-François Chatal, MD, Research Unit, 211 INSERM, Institut de Biologie, 9 Quai Moncousu, Nantes 44035 Cedex 01, France.

MATERIALS AND METHODS

Patients

The following adult patients were eligible for entry into this study:

1. Patients with measurable persistent disease or local and/or metastatic recurrences of MTC after surgery, as assessed by elevated serum thyrocalcitonin (TCT) concentration and positive morphological imaging techniques, including US and/or CT and/or MRI.
2. Patients with documented primary SCLC or relapse after conventional first-line chemotherapy. Only those patients with CEA-positive immunostaining of primary tumor biopsy specimens, as determined by the immunoperoxidase technique, were eligible. Other eligibility requirements included an absence of chemotherapy and radiotherapy for at least 3 mo. All patients underwent morphological imaging techniques (US, CT or MRI) within 1 mo before injection of BsMAb. All patients gave written informed consent to the protocol, which was approved by the regional ethics committee.

Five patients with MTC and five with SCLC were studied (Table 1). All patients with MTC had undergone total thyroidectomy with removal of regional lymph nodes between 1978 and 1993. At the time of immunoscintigraphy (IS), all five had elevated TCT values, and three had increased CEA values. The extent of the disease varied greatly among the patients (Table 2). Two had a large tumor burden—a mediastinal mass associated with a pulmonary metastasis in Patient 1 and a bulky liver metastasis in Patient 2, whereas cervical or liver recurrences were limited in Patients 3, 4 and 5.

All patients with SCLC except Patient 10 had been treated before IS (chemotherapy associated or not with external-beam radiation). The extent and site of the residual and/or recurrent tumor were variable (Table 2).

Bispecific Antibody Preparation and Bivalent Hapten Iodination

An anti-CEA/anti-In DTPA BsMAb designated as F6-734 (F6-734 BsMAb) was provided by Immunotech Pharma (Marseille, France) with a concentration of 0.68 mg/ml. Briefly, this BsMAb was obtained by coupling an equimolecular quantity of a Fab' fragment of an anti-CEA MAb (F6) to a Fab fragment of an anti-DTPA-indium MAb (734) activated beforehand by a maleimide function.

TABLE 1
Patient Characteristics

Patient no.	Sex	Age (yr)	MTC/SCLC	Previous treatment(s)	TCT (pg/ml)	NSE (ng/ml)	CEA (ng/ml)
1	M	62	MTC	S	24,264	—	107
2	F	48	MTC	S	377,880	—	4712
3	M	46	MTC	S	14,000	—	32
4	F	56	MTC	S	3480	—	5.7
5	M	69	MTC	S, RT	393	—	3.8
6	M	61	SCLC	RT, PCT	—	8.5	2.7
7	M	56	SCLC	RT, PCT	—	9.4	6.9
8	F	60	SCLC	PCT	—	5.7	2.5
9	M	44	SCLC	RT, PCT	—	7.8	22.8
10	M	57	SCLC	none (primary tumor)	—	27	77

MTC = medullary thyroid cancer; SCLC = small-cell lung cancer; S = surgery; RT = radiotherapy; PCT = polychemotherapy; TCT = thyrocalcitonin; NSE = neuron specific enolase; CEA = carcinoembryonic antigen.
Normal ranges: TCT < 10 pg/ml; CEA < 6 ng/ml; NSE < 12 ng/ml.

The bivalent hapten used was N-α-(diethylenetriamine-N,N,N',N''-tetraaceticacid-N''-acetyl)-tyrosyl-Nε-(diethylenetriamine-N,N,N',N'' tetraaceticacid-N''-acetyl) lysine (di-DTPA-TL) obtained by reaction of dianhydride of diethylenetriamine pentaacetic acid (DTPA) with tyrosyl-lysine diacetate (*3*).

The affinity of BsMAb was 4 10^9 M^{-1} to DTPA-indium at 37°C (*3*) and 2.1 10^9 M^{-1} to CEA as measured on LS174T cells (*4*).

Hapten Labelling with Iodine-131

Hapten labeling was performed according to the chloramine-T method. Briefly, 25 μl of a sterile solution of sodium ^{131}I (15.91 GBq/ml or 430 mCi/ml) and 30 μl of a sterile solution of chloramine-T (1 mg/ml) were added to 6 nmole of di-DTPA-TL in which indium had been previously chelated. After a 2-min incubation at room temperature, the oxidation reaction was stopped by addition of 30 μl of a sterile solution of sodium metabisulfite (1 mg/ml). After 5-min incubation, the solution was buffered (pH 5.6) by adding 815 μl of a sterile buffer solution of N-2-hydroxyethyl piperazine N'-2-ethane sulfonic acid (HEPES) 1 M, pH 5.6.

Purification of the ^{131}I-labeled di-DTPA In-TL solution obtained

TABLE 2
Imaging Results

Patient no.	Documented tumor sites	Scintigraphic imaging: Tumor visualization	Tumor uptake at Day 3 (%ID/g)	Tumor effective half-life (hr)	Liver effective half-life (hr)	Kidney effective half-life (hr)
1	Mediastinal mass	†	0.006	68	53	45
	right lung nodule	‡	0.004	51		
2	Liver mass	†	0.003	104	na	na
	right neck lymph nodes	—				
3	3 liver nodules:					
	Segment IV	‡	0.116	119	na	62
	Segment VII	—				
	Segment V	‡	na			
4	Right neck lymph nodes	†	0.108	146	75	89
		†	0.074	73		
5	Right neck lymph node	†	0.100	83	159	84
6	Left lung,	†	0.002	61	na	52
	mediastinal mass	§	0.003	132		
7	Left lung	—			47	35
	3 liver nodules:					
	Segment IV	§	na	na		
	Segment VIII	—				
	Segment VIII	—				
8	Right lung,	†	na	na	48	38
	left lung,	†	na	na		
	adrenal gland*,	—				
	brain	—				
9	Right adrenal gland*,	—				
	left adrenal gland	‡	0.009	80	58	65
10	Left lung (primary tumor)	‡	0.002	47	66	48

*Clinical course did not confirm malignant nature; † highly contrasted; ‡ moderately contrasted; § weakly contrasted.
na = nonassessable.

was performed by reverse-phase chromatography on Sep-Pak C18 cartridges (Waters, Milford, MA). The solution was injected into a cartridge previously conditioned by successive injections of 20 ml of ethanol and 10 ml of sterile HEPES buffer 0.1 *M*, pH 5.6. Free ^{131}I was eliminated in the column by injection of 10 ml of HEPES buffer 0.1 *M*, pH 5.6. The residual buffer contained in the column was then eliminated by successive injections of 1 ml of water and 5 ml of sterile air. The radiolabeled hapten was then eluted by injection of 3 ml of ethanol.

After the purification step, the activities of the ethanolic hapten solution, the buffered solution containing free iodine and the purification cartridge were measured, and the quantity of iodine bound by hapten was estimated from these results and from the specific activity of the ^{131}I solution used for labeling (168.72 TBq/g or 4560 Ci/mg).

The hapten solution was considered to be correctly radiolabeled each time the ratio of the ethanolic solution to the total activity deposited on the purification column was greater than 60%. In these conditions, the mean number of iodine atoms bound per molecule of hapten was estimated as two.

Immunoreactivity

To test the immunoreactivity of ^{131}I-labeled hapten, 5 μl of the ethanolic solution were diluted 1:2000 in buffer (pH 5) containing sodium acetate (100 m*M*), trisodium citrate (10 m*M*) and bovine serum albumin (BSA, 1 g/liter). A volume of 300 μl of this solution was transferred in duplicate into tubes coated with MAb 734 (anti-DTPA-In). After stirring at room temperature for 1 hr, the total activity deposited in each tube was measured in a gamma counter. The tubes were then emptied and washed three times with NaCl/Tween solution. Bound radioactivity was measured again in the same conditions as before. Immunoreactivity, defined as the ratio of bound activity after washing to total deposited activity, was considered satisfactory when the ratio was greater than 80%.

Two-Step Procedure

In a first step, 0.1 to 0.3 mg/kg of nonradiolabeled F6-734 BsMAb was injected by slow intravenous infusion over 20 min (0.09 to 0.1 mg/kg in patients with SCLC and 0.2 to 0.3 mg/kg in those with MTC). After 4 days, 6 nmole of ^{131}I-labeled di-DTPA In-TL (216 to 363 MBq or 5.8 to 9.8 mCi) were injected. Prior to this second injection, patients received 30 drops of Lugol's solution each day, beginning 24 hr before hapten injection and continuing for 3 wk.

Pharmacokinetic Study

Pharmacokinetic analysis was performed according to a methodology previously used, relative to a three-compartmental open model (*6,7*).

All parameters were calculated from this model using appropriate software. Blood samples were drawn before injection of ^{131}I-labeled hapten and then 5, 15, 30 min and 1, 5, 24, 48, 72, 96 and 168 hr after injection. Urine was collected between 0 and 5 hr, 5 and 24 hr and 24 and 72 hr. The radioactivity of blood and urine samples was measured in a gamma counter at Day 7 together with a decay standard. Statistical study of the results (variance analysis) was performed using appropriate software.

Scintigraphic Imaging and Dosimetric Studies

Cumulative activity in whole body, tumor, liver and kidneys was determined by whole-body quantitative scintigraphy performed with a two-headed camera equipped with a high-energy collimator, as proposed by DeNardo et al. (*8*). Whole-body scintigraphic images (anterior and posterior views) were recorded 5 min after injection of ^{131}I-labeled hapten and then at day 1, 2, 3, 4 and 7 using a 20% window set on the ^{131}I photopeak. The positioning of the patient was done in a reproducible manner using a system based on laser sources.

The attenuation corrective factor (ACF) was determined from a transmission image. A collimated linear source perpendicular to the direction of scanning movement was attached to the lower camera head. Acquisition was performed in the presence and then in the absence of the patient on the day of nonradiolabeled F6-734 BsMAb injection, thus defining the geometrical parameters for recordings.

The images were transferred to a Macintosh microcomputer where they were processed using two commercially available programs: Transform (Spyglass, Savoy, IL) and MedVision (Evergreen Technology, Castine, ME). The images acquired in 2048 × 512 format were compressed by summation of pixels to 512 × 128 to provide a format more comparable to the spatial resolution of the high-energy collimator and camera system used. The geometrical mean of each acquisition was calculated and multiplied by the ACF to obtain the resulting image. During each acquisition, a known activity standard was placed at the level of the patient's feet in order to determine the calibration factor for the camera (in counts per MBq in the air).

The activity A(t), in μCi, at each time point t was calculated according to the formula:

$$A(t) = \sqrt{I_{Ant} \cdot I_{Post}} \times ACF \times \frac{f}{C}$$

with

$$ACF = e^{\mu_{eff} L/2} = \sqrt{\frac{I_0}{I}},$$

where I_{Ant} and I_{Post} represent, pixel by pixel, the counts obtained in anterior and posterior views, f the autoattenuation factor of the source (in our study, $f \approx 1$) and C the calibration coefficient for the camera (in counts/μCi). I_0 and I are the counts obtained pixel by pixel on the transmission image in the absence and then the presence of the patient, respectively.

As corrections were performed before regions of interest (ROIs) were defined, the activity on the resulting image was determined by:

$$A(t) = I_{Res}/C,$$

where I_{Res} represents, pixel by pixel, the counts obtained resulting image.

The activities calculated at the different time points were transferred into a pharmacokinetic study program (Siphar, Simed) to determine the effective half-lives of ^{131}I-labeled hapten in the regions defined and then the cumulative activity. In Patients 4 and 5, the activity estimated by quantitative scintigraphy was compared with that of the entire surgically resected tumor measured in a well counter (at Day 7 for Patient 4 and at Day 8 for Patient 5).

The doses absorbed by tumor targets and normal tissues after injection of ^{131}I-labeled hapten were calculated according to the MIRD scheme (*9*). The absorbed dose was defined by:

$$\bar{D}_{(t \leftarrow s)} = \tilde{A} \frac{\Delta \phi_{(t \leftarrow s)}}{m_t},$$

where $\bar{D}_{(t \leftarrow s)}$ is the dose (Gy) delivered to the target t by the source s, $\tilde{A}$ the cumulative activity (MBq.sec or μCi.hr), Δ the constant of the radionuclide dose (g.cGy/μCi.hr) and ϕ the fraction of energy emitted by the source and absorbed by the target mass m_t (g). In the case of ^{131}I and for sources with a diameter greater than 1 cm, $\phi = 1$ for beta emissions. Tumor target mass was estimated from CT scan sections with a thickness of 5 mm or 1 cm or, for Patients 4 and 5 determined precisely by weighing the resected tumors.

Dosimetry was performed on scintigraphically visualized tumors for which it was possible to define a target volume (and thus

estimate the mass) from CT scan sections. Due to the partial volume effect, the volumes of the tumors were estimated to have a relative accuracy of 20%. The mass of normal tissues (liver and kidney) was estimated by reference values. ROIs were defined on the liver and left kidney of each patient in order to estimate the doses delivered to these organs.

The calculation of the bone marrow dose was performed according to the technique of De Nardo et al. (*10*) by summing a whole-body component of the bone marrow dose (only penetrating radiations are taken into account) and a blood component (only nonpenetrating radiations are taken into account).

Detection of Anti-Mouse Antibodies

Anti-mouse antibodies (HAMA) were assessed according to a previously described procedure (*4*). Briefly, human anti-bispecific antibody concentration was determined in duplicate from patients' sera using a one-step double antigen sandwich radioimmunoassay on F6-734 BsMAb-coated tubes.

RESULTS

Hapten Labeling

The di-DTPA In-TL hapten labeling technique was reproducible. Labeling efficiency showed little variation (between 60% and 68%), and immunoreactivity ranged from 91% to 99%.

Tumor Imaging

All patients with MTC had positive IS results (Table 2). Tumors were clearly visualized at 24 hr in patients with various TCT and/or CEA serum concentrations, various localizations and various burdens, but contrast was increased at Days 5 or 7 due to a reduction in adjacent nonspecific activity (Fig. 1). Relative to conventional morphological imaging, IS visualized an additional tumor site in Patient 4 who underwent surgery after IS (Fig. 2). The smallest visible tumor (a right neck lymph node resected in Patient 5) weighed 0.8 g.

IS was clearly positive in four of the five SCLC patients but all documented tumor sites were not visualized in two of these four patients; for Patient 6, a large hot spot was visualized early in the left lung (at Day 0), and high contrast was observed from Days 3 to 7. This large tumor, later confirmed by CT scan, was estimated to weigh about 125 g. An additional mediastinal mass, not previously documented, was visualized on an IS anterior planar view and subsequently confirmed by CT from which volume could be estimated. IS was falsely negative for Patient 7 in three documented tumor sites and weakly positive in a small liver metastasis. For Patient 8, IS was clearly positive in a large recurrence infiltrating both lungs, but the volume could not be even roughly estimated on CT. For the same patient, IS failed to visualize cerebral metastases and hypertrophic adrenal glands. Under polychemotherapy, lung tumors regressed in size, whereas the hypertrophic adrenal glands remained unchanged (presumably nonmetastatic). For Patient 9, IS imaged one (left) of the enlarged adrenal glands visualized on CT (Fig. 3). Under polychemotherapy the left adrenal tumor regressed in size, whereas no change occurred in the right adrenal mass (presumably nonmetastatic).

Pharmacokinetic Study

The results of the pharmacokinetic study are reported in Table 3. Mean distribution half-lives ($T_{1/2}$ α, β and γ) and mean residence time for all 10 patients were 0.50 ± 0.24 hr, 7.71 ± 2.95 hr and 63.72 ± 21.68 hr, respectively. The corresponding pre-exponential values (mCi/liter) were 0.376 ± 0.096, 0.185 ± 1.196 and 1.184 ± 0.345, respectively. Mean residence time for all 10 patients was 66.66 ± 13.40 hr. Two of the 10 patients (Patients 4 and 7) presented pharmacokinetic parameters which could only be analyzed using a two-compartmental open model.

Values for equilibrium distribution volume, elimination half-lives and clearances (blood and urine) in patients with MTC (injected BsMAb: 0.3 mg/kg) and SCLC (injected BsMAb: 0.1 mg/kg) were significantly different: 14.89 ± 7.71 l versus 64.01 ± 31.54 l ($p < 0.01$); 49.63 ± 13.73 versus 77.82 ± 19.28 hr ($p < 0.03$); 0.27 ± 0.18 $l \cdot hr^{-1}$ versus 0.90 ± 0.46 $l \cdot hr^{-1}$ ($p < 0.02$) and 0.21 ± 0.17 $l \cdot hr^{-1}$ versus 0.74 ± 0.24 $l \cdot hr^{-1}$ ($p < 0.004$), respectively.

The mean fraction (±s.d.) of activity excreted in urine was 20.7 ± 9.0% from 0 to 5 hr, 20.2 ± 5.1% from 5 to 24 hr and 12.9 ± 6.1% from 24 to 72 hr in patients with MTC, and 45.4 ± 4.0% from 0 to 5 hr, 25.0 ± 5.0% from 5 to 24 hr and 5.7 ± 3.6% from 24 to 72 hr in patients with SCLC.

Dosimetric Studies

The results for dosimetric studies are shown in Table 4. The dosimetric approach was validated on a phantom by determining the optimal protocol for quantitative scintigraphy. Real activity was assessed in spherical sources of different volume (0.5 to 10 ml) simulating tumors or in sources of greater volume simulating organs (150-ml container of physiological serum simulating a kidney, 3-liter cylinder simulating a liver) immersed in an oval 15-liter tank, with or without background noise, simulating the abdominal cavity.

The ACF was calculated for each patient. The correction for each image pixel varied between 1.5 and 3 according to the patient and the anatomical regions considered.

The activity in each ROI was determined from the standard source positioned in the air next to the patient during acquisition, except for whole-body activity, which was determined from the percentage of counts obtained 10 min after injection on Day 0, taken as the reference. As reported in Table 2, tumor effective half-lives ranged from 51 to 146 hr for MTC patients and from 47 to 132 hr for SCLC patients. Liver and kidney effective half-lives ranged from 53 to 159 hr and 45 to 89 hr for MTC patients and from 47 to 66 hr and 35 to 65 hr for SCLC patients, respectively. The results for tumor uptake, expressed in %ID/g at Day 3, as a function of tumor mass, are shown in Figure 4. It is quite apparent that tumor uptake was much higher (on an order of magnitude) for small tumors weighing about 1 g than for those weighing more than 10 g.

For three small nodules, activities obtained by quantitative imaging were compared with those obtained by counting resected tumors. For Patient 4, the activity in two right neck lymph nodes (weighing 1.15 g and 0.83 g as assessed after resection) was 5.1 and 2.7 μCi at Day 7, respectively. Activities calculated at Day 6 from quantitative imaging were 6.4 and 3 μCi, respectively. For Patient 5, the activity in a right neck lymph node (0.80 g as assessed after resection) was 3.3 μCi at Day 8. Activity calculated at Day 7 from quantitative imaging was 4.1 μCi. This good agreement validates our quantitative imaging protocol.

For patients with MTC, tumor-to-blood ratios ranged from 0.6 to 69.1 (Fig. 5). If we exclude the 0.6 value (Patient 2), attributable to a very elevated serum CEA concentration leading to the formation of radioactive immune complexes, the mean value was 41. Tumor-to-liver ratios ranged from 7.6 to 125.5 (mean: 51), and tumor-to-kidney ratios from 1.4 to 39.4 (mean: 13). For patients with SCLC, tumor-to-blood ratios ranged from 3.4 to 18.8 (mean: 11), tumor-to-liver ratios from 8.1 to 14.5 (mean: 8.4) and tumor-to-kidney ratios from 0.2 to 6.5 (mean: 2.7).

For tumor targets, absorbed doses ranged between 1.7 cGy/

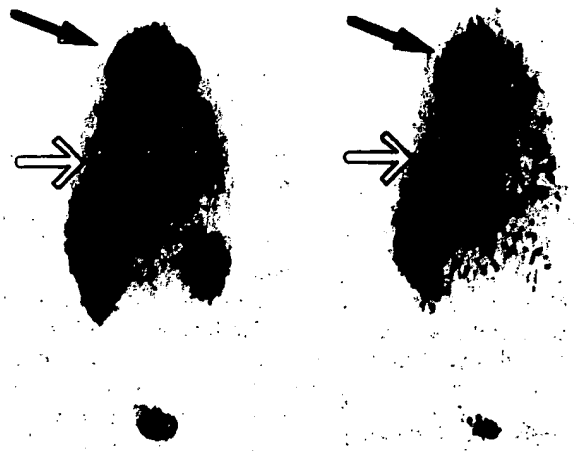

Day 3 Day 7

FIGURE 1. Whole-body anterior views of Patient 1 obtained 3 and 7 days after injection of ^{131}I-labeled hapten (7 and 11 days after a first injection of BsMAb). Clear visualization of a 125 cm^3 mediastinal recurrence (closed arrow) and a 10 cm^3 right lung metastasis (open arrow).

mCi for Patient 10 with a primary tumor and 174 cGy/mCi for Patient 3 with a liver metastasis (Table 4).

To calculate the doses delivered to the liver and left kidney, the contours of these organs were sketched on the images, except when the liver was indistinguishable from liver metastases (Patients 2 and 3) or when high circulating activity prevented clear imaging of the kidney (Patient 2). Doses were calculated by

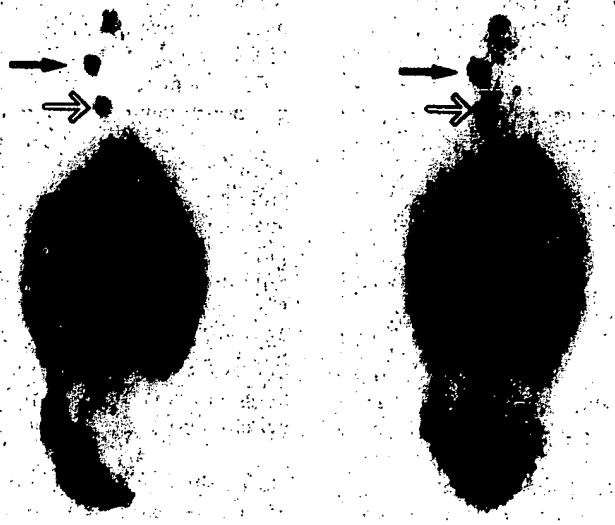

Day 3 Day 7

FIGURE 2. Whole-body anterior views of Patient 4 obtained 3 and 7 days after injection of ^{131}I-labeled hapten (7 and 11 days after a first injection of BsMAb). Highly contrasted visualization of two 1.15 g (closed arrow) and 0.83 g (open arrow) right neck recurrences surgically resected 7 days after hapten injection.

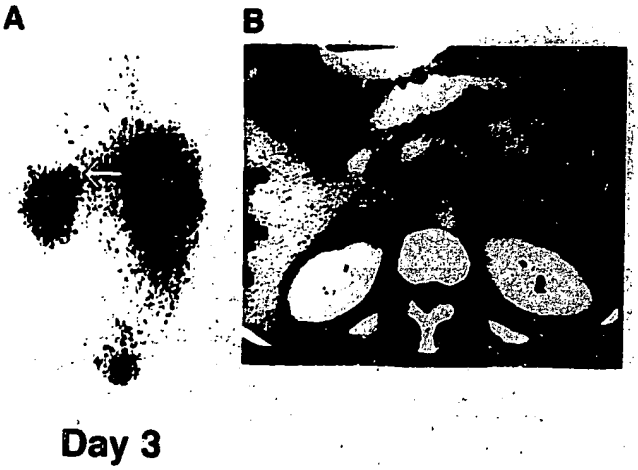

Day 3

FIGURE 3. (A) Posterior abdominal view of Patient 9 obtained 3 days after injection of ^{131}I-labeled hapten (7 days after a first injection of BsMAb). A hot spot is visualized in the left suprarenal area (open arrow). (B) Abdominal CT scan shows bilateral adrenal masses. Left adrenal mass (open arrow) has a 11 ± 2 cm^3 volume.

assuming a mean mass of 1800 g for the liver and 120 g for the kidney. Doses between 0.2 and 4.3 cGy/mCi were computed for liver and between 1.3 cGy/mCi and 9 cGy/mCi for kidney.

Bone marrow absorbed doses, calculated from sketched contours (whole-body component) and results of blood kinetics, were between 0.2 and 1.5 cGy/mCi. Blood absorbed doses ranged between 0.1 and 1.1 cGy/mCi.

Detection of Anti-Mouse Antibodies

HAMA was positive for three of the five patients with MTC: One early detection 15 days after BsMAb injection (Patient 5) and two later detections at day 90 (Patients 1 and 3). HAMA was positive during the first month after BsMAb injection in two of the five patients with SCLC.

DISCUSSION

The results of this study confirm those previously obtained with the same BsMAb and ^{111}In-labeled bivalent hapten, showing favorable tumor uptake values and tumor-to-normal tissue ratios for RIT applications. In patients with colorectal carcinomas, tumor uptake values were the same for the one- and two-step techniques, but tumor-to-blood and tumor-to-liver ratios were 1.9- to 3.5-fold higher with the latter technique (*4*). In the same clinical situation of colorectal carcinoma, very high tumor uptake values (greater than 0.1% ID/g), comparable to those for MTC patients in our study, have been found when an anti-CEA antibody directly labeled with ^{131}I was used for small tumor targets of less than 10 g (*11*). For MTC patients in the present study, tumor-to-normal tissue ratios were above 50 in two patients and above 10 in six. The only value below 1 was obtained in Patient 2 with a tumor mass weighing 500 g and a very high serum CEA concentration. In comparison, two studies (concerning a limited number of patients) have reported tumor-to-normal tissue ratios lower than 5 when an anti-CEA antibody directly labeled with ^{111}In was used (*12,13*).

In our study, a three-compartmental open model appeared to be the most suitable choice for pharmacokinetic analysis, in accordance with theoretical data published by Baxter et al. (*7*) and comments concerning the limitations of a two-compartmental model (*6*). Based on data reported by Le Doussal et al. (*4*), who used the same BsMAb and the same ^{111}In-labeled hapten, we found shorter distribution half-lives than those obtained when a directly labeled antibody was used (less than 30 min on average

TABLE 3
Pharmacokinetic Analysis According to a Three-Compartment Model

Patients	$T_{1/2}\ \alpha$ (hr)	$T_{1/2}\ \beta$ (hr)	$T_{1/2}\ \gamma$ (hr)	VDss (l)	MRT (hr)	Blood cl. ($l \cdot hr^{-1}$)	Urin. cl. ($l \cdot hr^{-1}$)	AUC ($mCi \cdot hr \cdot l^{-1}$)
MTC								
1	0.79	11.78	65.57	28.06	48.82	0.57	0.49	13.27
2	0.84	9.53	60.81	7.74	84.60	0.09	0.05	97.90
3	0.22	3.26	45.78	12.75	63.72	0.20	0.17	22.95
4	0.68	—	31.29	13.75	43.86	0.31	0.22	22.01
5	0.12	3.89	44.70	12.16	62.24	0.19	0.11	40.70
mean	0.53	7.11	49.63	14.89	60.65	0.27	0.21	39.36
$\pm\sigma$	±0.33	±4.20	±13.73	±7.71	±15.87	±0.18	±0.17	±34.21
SCLC								
6	0.40	6.46	88.41	110.52	70.88	1.56	0.84	4.77
7	0.60	—	59.75	26.05	85.27	0.30	0.31	22.14
8	0.40	9.40	106.28	73.35	74.64	0.98	0.84	7.90
9	0.37	8.26	64.26	47.03	66.21	0.71	0.76	11.56
10	0.62	9.10	70.42	63.12	66.42	0.95	0.93	9.02
mean	0.48	8.30	77.82	64.01	72.68	0.90	0.74	11.08
$\pm\sigma$	±0.12	±1.32	±19.28	±31.54	±7.85	±0.46	±0.24	±6.64

MTC = medullary thyroid cancer; SCLC = small-cell lung cancer; VDss = steady-state distribution volume; MRT = mean residence time; cl = clearance; AUC = area under the curve; ns = nonsignificant.

for the two-step system in our study versus more than 2 hr for a directly labeled antibody (*14,15*)). The elimination kinetics study showed no significant differences between the one- and two-step systems. The mean residence times found in our study show that the values obtained are close to those for elimination half-lives. This would seem to confirm that the radioactivity elimination step after injection of ^{131}I-labeled hapten is limited owing to the elimination of circulating hapten-BsMAb complexes.

Studies were conducted on a phantom to validate the dosimetric protocol. The effect of patient volume on photon scatter and quantification of activity present in tumor and normal tissues was studied for increasing source volumes (unpublished data). The results show that error during determination of the activity present in small sources (0.5 to 10 ml) was low (less than 10%) but could be high for large volumes (up to 200% for an oval 15-liter abdominothoracic phantom 22 cm thick). As total activity measurements were available for the tumors of Patients 4 and 5 after surgery. These results were compared with those obtained from scintigraphic images recorded before the operation and found to be in close agreement. It should be noted, however, that background activity subtraction was easier on late images, thus augmenting the accuracy of activity calculations.

Background noise before subtraction was estimated for each ROI based on the minimal count value in this zone. As the definition of a ROI is highly operator-dependent, all zones were sketched by the same persons (a physician assisted by a physicist). In these conditions, even though the precision of the calculated activity may be debatable, we sought to minimize operator-related differences between patients.

In the clinical situation of MTC, recurrences of tumor uptake values were correlated with the volume of the targets considered (Fig. 4), reaching a maximum value of 0.116 %ID/g at day three (Patient 3). These elevated tumor uptake values for small targets, which are comparable to those calculated by Siegel et al. (*11*) in patients with recurrences of colorectal cancer, may have been due to higher blood flow in smaller than larger tumors. Vaupel et al. (*16*) have in fact shown that blood flow decreases exponentially in relation to tumor mass. The doses delivered to tumors ranged from 4.2 to 174 cGy/mCi. By extrapolating these values to injected activities of 100 mCi,

TABLE 4
Dosimetric Calculations

Patient no.	Tumor mass (g)	Dose (cGy/mCi)					
		Tumor	Liver	Left kidney	Blood	(TR)	Bone marrow
1	125.0	4.8	0.5	2.6	0.3	(4.5)	0.5
	10.0	5.3				(5.0)	
2	500.0	4.2	na	na	1.1	(0.9)	1.5
3	1.8	174	na	8.1	0.3	(143.8)	0.6
4	1.15	125	1.1	9.0	0.3	(95.9)	0.6
	0.83	74				(56.5)	
5	0.80	135	4.3	2.5	0.5	(63.1)	0.9
6	315.0	1.9	0.5	1.6	0.07	(6.7)	0.2
	15.0	3.9				(13.7)	
7	—	—	0.3	2.9	0.2		0.4
8	—	—	0.2	5.1	0.1		0.2
9	12.0	8.0	0.4	1.3	0.2	(13.1)	0.3
10	40.0	1.7	0.4	6.1	0.1	(3.8)	0.2

na = nonassessable; TR = therapeutic ratio; $\tilde{C}_{Tumor}$ (μCi·hr/g)/$\tilde{C}_{Blood}$ (μCi·hr/ml).

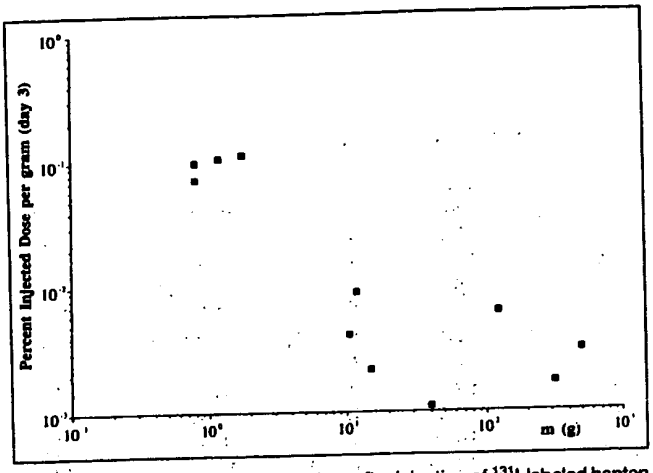

FIGURE 4. Tumor uptake (%ID/g) 3 days after injection of ^{131}I-labeled hapten versus tumor weight.

comparable to the activity of ^{131}I administered for treatment of metastases of differentiated thyroid carcinoma, absorbed tumor doses of 135 and 174 Gy would be obtained for a cervical metastasis of 0.8 g (Patient 5) and a liver metastasis of 1.8 g (Patient 3), respectively. Much lower doses (less than 10 Gy) would be delivered to large tumors (Patients 1 and 2). Thus, these results confirm the commonly accepted opinion that RIT is maximally efficient for small tumors, particularly micrometastases (*17*). The potential interest of this approach can be evaluated relative to the clearly established use of internal radiotherapy with ^{131}I for metastases of differentiated thyroid carcinoma, even though the radiosensitivity of the two types of cancer is not the same. The absorbed tumor dose values computed in this study are comparable to those reported by Thomas et al. (*18*) for cervical metastases (43 to 140 cGy/mCi for tumors weighing 8 to 40 g).

In the clinical situation of SCLC recurrences, tumor uptake values were much lower than for MTC recurrences, reaching a maximum value of 0.009 %ID/g for a tumor weighing about 12 g (Patient 9). Although patients were included in the study on the basis of CEA expression by cells of their primary tumor, as evaluated by immunohistochemical analysis of biopsy material, it is possible that the recurrences themselves expressed less CEA, which could account for the relatively low tumor uptake values. Moreover, tumor volume was generally higher, and the mean quantity of BsMAb injected was one-third of that administered to patients with MTC, which could also account for the lower uptake values. Irradiation doses, estimated between 1.9 and 8 cGy/mCi in the 5 patients, are comparable to those estimated for a variety of ^{131}I-labeled antibodies in patients with refractory forms of lymphoma presenting radiosensitivity comparable to that of SCLC (*19–21*).

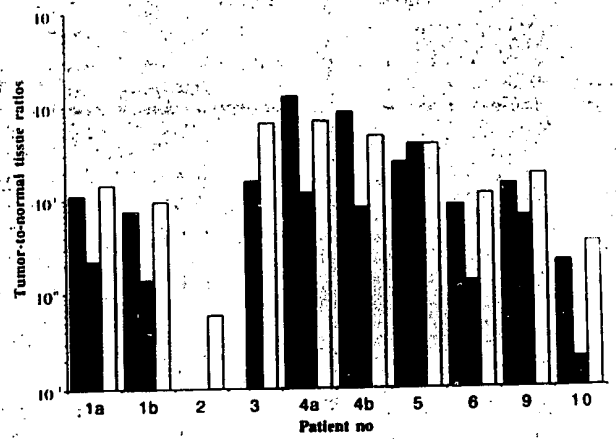

FIGURE 5. Tumor-to-normal tissue ratio as determined by quantitative scintigraphy: tumor-to-liver (black), tumor-to-kidney (gray), tumor-to-blood (white).

CONCLUSION

A two-step pretargeting system using anti-CEA/anti-DTPA indium BsMAb and a ^{131}I-labeled di-DTPA In-TL bivalent hapten allowed us to obtain high tumor uptake and absorbed dose values for small MTC recurrences. For SCLC recurrences, the values of the same parameters were lower but in the same range as those obtained by other investigators with the one-step technique in refractory lymphoma.

ACKNOWLEDGMENT

This work was supported by a grant from the Programme Hospitalier de Recherche Clinique 1994 conducted by the French Ministry of Health.

REFERENCES

1. Kaminski MS, Zasadny KR, Francis IR, et al. Radioimmunotherapy of B-cell lymphoma with [^{131}I]-anti-B1 (anti-CD 20) antibody. *N Engl J Med* 1993;329:459–465.
2. Press OW, Eary JF, Appelbaum FR, et al. Radiolabeled-antibody therapy of B-cell lymphoma with autologous bone marrow support. *N Engl J Med* 1993;329:1219–1224.
3. Le Doussal JM, Gruaz-Guyon A, Martin M, et al. Targeting of indium-111-labeled bivalent hapten to human melanoma mediated by bispecific monoclonal antibody conjugates: imaging of tumors hosted in nude mice. *Cancer Res* 1990;50:3445–3452.
4. Le Doussal JM, Chetanneau A, Gruaz-Guyon A, et al. Bispecific monoclonal antibody mediated targeting of an indium-111-labeled DTPA dimer to primary colorectal tumors: pharmacokinetics, biodistribution, scintigraphy and immune response. *J Nucl Med* 1993;10:1662–1671.
5. Peltier P, Curtet C, Chatal JF, et al. Radioimmunodetection of medullary thyroid cancer using a bispecific anti-CEA/anti-Indium-DTPA antibody and an indium-111-labeled DTPA dimer. *J Nucl Med* 1993;34:1267–1273.
6. Yuan F, Baxter LT, Iain RK. Pharmacokinetic analysis of two-step approaches using bispecific and enzyme-conjugated antibodies. *Cancer Res* 1991;51:3119–3130.
7. Baxter LT, Yuan F, Jain RK. Pharmacokinetic analysis of the perivascular distribution of bispecific antibodies and haptens: comparison with experimental data. *Cancer Res* 1992;52:5838–5844.
8. DeNardo GL, DeNardo SJ, Macey DJ, et al. Quantitative pharmacokinetics of radiolabeled monoclonal antibodies for imaging and therapy in patients. In: Srivastava SC, ed. *Radiolabeled monoclonal antibodies for imaging and therapy*. New York: Plenum; 1988:293–309.
9. Loevinger R, Budinger TF, Watson EE. MIRD primer for absorbed dose calculations. Society of Nuclear Medicine, 1988.
10. DeNardo GL, Mahé MA, DeNardo SJ, et al. Body and blood clearance and marrow radiation dose of ^{131}I-Lym-1 in patients with B-cell malignancies. *Nucl Med Com* 1993;14:587–595.
11. Siegel JA, Pawlyk DA, Lee RE, et al. Tumor, red marrow and organ dosimetry for ^{131}I-labeled anti-carcinoembryonic antigen monoclonal antibody. *Cancer Res* 1990; 50:1039s–1042s.
12. Reiners C, Eilles C, Spiegel W, et al. Immunoscintigraphy in medullary thyroid cancer using an ^{123}I- or ^{111}In-labeled monoclonal anti-CEA antibody fragment. *J Nucl Med* 1986;25:227–231.
13. Edington HD, Watson CG, Levine G, et al. Radioimmunoimaging of metastatic medullary carcinoma of the thyroid gland using an indium-111-labeled monoclonal antibody to CEA. *Surgery* 1988;104:1004–1010.
14. Hnatowich DJ, Gionet M, Rusckowski M, et al. Pharmacokinetics of ^{111}In-labeled OC-125 antibody in cancer patients compared with the 19-9 antibody. *Cancer Res* 1987;47:6111–6117.
15. Kinuya S, Jeong JM, Garmestani K, et al. Effect of metabolism on retention of Indium-111-labeled monoclonal antibody in liver and blood. *J Nucl Med* 1994;35: 1851–1857.
16. Vaupel P. Oxygen supply to malignant tumors. In: Petersen HI, ed. *Tumor blood circulation, angiogenesis, vascular morphology and blood flow of experimental and human tumors*. Boca Raton: CRC Press; 1979:143.
17. Zanzonico P. Radioimmunotherapy of micrometastases: a continuing evolution. *J Nucl Med* 1992;33:2180–2183.
18. Thomas SR, Maxon HR, Kereiakes JG, et al. Quantitative external counting techniques enabling improved diagnostic and therapy decisions in patients with well-differentiated thyroid cancer. *Radiology* 1977;122:731–737.
19. Eary JF, Press OW, Badger CC, et al. Imaging and treatment of B-cell lymphoma. *J Nucl Med* 1990;31:1257–1268.
20. Goldenberg DM, Horowitz JO, Sharkey RM, et al. Targeting, dosimetry and radioimmunotherapy of B-cell lymphoma with iodine-131-labeled LL2 monoclonal antibody. *J Clin Oncol* 1991;9:548–564.
21. Kaminski MS, Fig LM, Zasadny KR, et al. Imaging, dosimetry and radioimmunotherapy with iodine-131-labeled anti-CD 37 antibody in B-cell lymphoma. *J Clin Oncol* 1992;10:1696–1711.

INTER LIBRARY LOAN REQUEST FORM

Borrower's Name: D. SAUNDERS | Org. or A.U.: 1644 | Phone: 308-3976

Serial Number: 337,756 | Date of Request: 2/7/01 | Date Needed By: 2/12/01

Please Attach Copy Of Abstract, Citation, Or Bibliography, If Available. Please Provide Complete Citation. Only One Request Per Form.

Author/Editor: GAUTHEROT et al

Journal/Book Title: JOUR. OF NUCLEAR MEDICINE

Article Title: DELIVERY OF THERAPEUTIC ...

Volume (Issue): 39 (11)

Pages: 1937-1943

Year of Publication: 1998

Publisher:

Remarks:

NLM A pubs

STIC Use Only RM 845. J78 M&C

Accession Number: _____

LIBRARY ACTION	LC		NAL		NIH		NLM		NBS		PTO		OTHER	
	1st	2nd	1st	2nd	1st	2nd	1st	2nd	1st	2nd	1st	2nd	1st	2nd
Local Attempts														
Date														
Initials														
Results														
Examiner Called														
Page Count														
Money Spent														

Provided By: Source and Date

Ordered From: Source and Date

Remarks/Comments

1st & 2nd denotes time taken to a library

O/N - Under NLM means Overnight Service

FX - Means Faxed to us

Delivery of Therapeutic Doses of Radioiodine Using Bispecific Antibody-Targeted Bivalent Haptens

Emmanuel Gautherot, Jean-Marc Le Doussal, Jamila Bouhou, Corine Manetti, Marie Martin, Eric Rouvier and Jacques Barbet
Immunotech SA, Marseille and Hopital Pitie-Salpetriere, Laboratoire d'Immunologie Cellulaire, Paris, France

Two-step pretargeting strategies have been designed to deliver radioisotopes to tumors more selectively than directly labeled antibodies or fragments. In this article, we compare quantitatively the potential of these strategies for the radioimmunotherapy of solid tumors. **Methods:** Direct targeting was performed using iodine-labeled IgG and $F(ab')_2$. As two-step strategies, we used the sequential injection of anti-CEA × anti-DTPA-In bispecific $F(ab')_2$ ($BsF(ab')_2$) and monovalent and bivalent DTPA derivatives labeled with iodine. The biodistribution of iodine in nude mice grafted with the LS174T human colorectal carcinoma was monitored in time and used for calculating radiation doses. **Results:** In agreement with earlier studies, the IgG was more effective for delivering a radiation dose to the tumor than the $F(ab')_2$ (7.8 versus 0.76 Gy/MBq, respectively) and both were moderately selective with respect to normal tissues (tumor:blood of 2.9 and 1.7, respectively). At their MTD, they should deliver 86 and 34 Gy, respectively, to the tumor. Using a nM-affinity DTPA-In bivalent hapten, the two-step protocol was optimized by varying the dosage of the $BsF(ab')_2$, the stoichiometry of the reagents and the pretargeting time. The saturation of the tumor was obtained by injecting 5 nmol (500 μg) of $BsF(ab')_2$. The pretargeted $BsF(ab')_2$ was saturated by the injection of 0.5 mol of bivalent hapten per mole of antibody. With a 48-hr pretargeting time, the selectivity of the irradiation of the tumor was optimized (tumor:blood of 7.8) but only at the price of a lower efficiency (0.35 versus 0.86 Gy/MBq, 48-hr and 20-hr pretargeting time, respectively). Attempts to increase selectivity by using a μM-affinity DTPA-Y bivalent hapten or by chasing excess circulating radiolabeled hapten with an excess of unlabeled hapten also reduced tumor exposure. The use of a monovalent hapten resulted in both lower efficiency and selectivity. However, the two-step pretargeting of high-affinity bivalent hapten (Affinity Enhancement System, AES) should deliver 30–60 Gy to the tumor with less than 9 Gy to the blood in tumor-bearing mice. **Conclusion:** Radioimmunotherapy with AES is predicted to be as efficient and with lower hematological toxicity than direct targeting.

Key Words: bispecific antibody; pretargeting; dosimetry; carcinoembryonic antigen; colon carcinoma; radioimmunotherapy

J Nucl Med 1998; 39:1937–1943

Radioimmunotherapy (RAIT) with ^{131}I-labeled monoclonal antibodies has yielded contrasting clinical results, depending on the target tumor. In the treatment of refractory B cell lymphomas, complete cures have been achieved (*1,2*). Only partial responses have been reported so far in solid tumors because of poorer accessibility and lower radiosensitivity (*3,4*). One of the main limitations of the RAIT of solid tumors is the secondary toxicity, especially to the hematopoietic system.

The targeting of small radiolabeled haptens (or biotin) to pretargeted bispecific antibody (or avidin-antibody conjugates) has been designed to improve tumor-to-normal tissue ratios (*5*). We have developed an improved pretargeting strategy, the Affinity Enhancement System (AES), where the hapten is bivalent, thus exhibiting higher avidity for cell-bound than for free-circulating bispecific antibody ($BsF(ab')_2$). AES reagents have been demonstrated to target iodine or indium more selectively to different experimental tumors (*6–8*). A similar improvement was shown in clinical trials of immunoscintigraphy of CEA-expressing tumors (*9*). Furthermore, a preliminary clinical dosimetry study showed that ^{131}I-labeled AES reagents delivered radiation doses to tumors in the range of those obtained using direct targeting (*10*).

Pretargeted radioimmunotherapy requires a careful optimization of the experimental protocols to achieve high and stable tumor localization combined with low normal tissue exposure. In the experiments reported here, we studied the respective influence of reagent doses, pretargeting time, valence and affinity of DTPA haptens for an anti-CEA × anti-DTPA $BsF(ab')_2$ on the AES pretargeting efficiency in nude mice grafted with LS174T human colorectal carcinoma. Optimized protocols with AES reagents were compared with direct targeting using IgG or $F(ab')_2$ in terms of dose delivery and selectivity.

MATERIALS AND METHODS

Human Colon Carcinoma Model in Nude Mice

The human colon carcinoma LS174T cell line was obtained from the Cell Distribution Center, American Type Culture Collection (Rockville, MD). Cells were grown in Dulbecco's modified Eagle's medium supplemented with 10% fetal bovine serum, 100 U/ml penicillin and 100 μg/ml streptomycin (Sigma, St. Louis, MO). Cells were harvested after incubation for 5 min with trypsin-EDTA (0.05%–0.02%) at 37°C. Exponentially growing tumor cells (2.5×10^6) were grafted into 10–12 wk-old female NMRI nude mice (CERJ, Le Genest, Saint Isle, France) by subcutaneous injection in the flank. Ten days later mice bearing tumors ranging from 20–200 mm^3 were selected for the experiments.

Monoclonal Antibodies, Fragments and Bispecific Antibody

Anti-CEA clone F6 and anti-DTPA-metal clone 734 are mouse IgG_1 from Imminotech (Marseille, France). Both antibodies were purified from ascites fluid by affinity chromatography on protein A-Sepharose (Pharmacia, Uppsala, Sweden). $F(ab')_2$ fragments were prepared by pepsin (Sigma) digestion (5% weight/weight, 2 hr at 37°C). The anti-CEA × anti-DTPA-metal bispecific antibody ($BsF(ab')_2$) was prepared by the chemical coupling of the two reduced Fab' fragments using *o*-phenylenedimaleimide according to the procedure described by Glennie et al. (*11*).

Bivalent Hapten Synthesis

The monovalent DTPA hapten N-α-acetyl-N-ε-diethylenetriaminepentaacetic acid-lysyl-D-tyrosyl-Nε-(glycyl-succinyl-histamine)-lysinamide (AG5.0) was synthesized, using solid-phase peptide synthesis, by Gruaz-Guyon (*12*).

The bivalent DTPA hapten N-α-diethylenetriaminepentaacetic acid-tyrosyl-N-ε-diethylenetriaminepentaacetic acid-lysine was prepared by reacting DTPA dianhydride with tyrosyl-lysine diac-

Received Oct. 14, 1997; revision accepted Feb. 23, 1998.
For correspondence or reprints contact: Emmanuel Gautherot, PhD, Immunotech SA, 130 avenue De Lattre de Tassigny BP 177 13276 Marseille Cedex 9, France.

etate and purified by size exclusion chromatography and reverse phase chromatography (*7*).

Clearing Agent

Human serum albumin substituted with an average of 35 mol galactose and 5 mol DTPA per mole (DTPA-HSA) was obtained from Nihon Medi-Physics (Tokyo, Japan).

Labeling

Antibodies (0.5 nmol IgG, $F(ab')_2$ or $BsF(ab')_2$) were labeled with 18.5 MBq ^{125}I (3.7 GBq/ml; Amersham, Les Ullis, France) or ^{131}I (14.8 GBq/ml; CIS bio International, Gif sur Yvette, France) using Iodo-Gen (Pierce, Rockford, IL). The reaction was stopped by the addition of 10 nmol D,L-tyrosine (Sigma) and labeled antibodies were separated from free iodine by gel filtration on a PD-10 column (Pharmacia).

The bivalent hapten was labeled with ^{111}In using 18.5 MBq $^{111}InCl_3$ (370 MBq/ml; Mallinckrodt, Petten, The Netherlands) for 1 nmol of hapten as already described (*9*). The bivalent hapten then was saturated by the addition of an excess of $InCl_3$.

For labeling with iodide, the monovalent hapten and the bivalent hapten were dissolved at 40 μM in 0.1 M acetate, 10 mM citrate, pH 5.5 and saturated with a 25-fold excess of the metal ion. The monovalent hapten was saturated with $InCl_3$ (referred to as mono-DTPA-In), whereas the bivalent hapten was saturated either with $InCl_3$ or with YCl_3 (referred to as di-DTPA-In and di-DTPA-Y, respectively). Di-DTPA-In, di-DTPA-Y and mono-DTPA-In hapten were then labeled by the chloramine T (Merck, Darmstadt, Germany) method, using 37 MBq sodium [^{125}I]iodide for 2 nmol of hapten. The labeled and unlabeled hapten were separated from free iodine by gel filtration on a PD-10 column. The specific activity was 6.7 MBq/nmol, 6.8 MBq/nmol and 8.0 MBq/nmol for di-DTPA-In, di-DTPA-Y and mono-DTPA-In, respectively.

DTPA-GSA was labeled using 18.5 MBq $^{111}InCl_3$ for 0.1 nmol of protein. After saturation with excess $InCl_3$, the labeled protein was purified by gel filtration on a PD-10 column.

Reagent Purity, Reactivity and Affinity

The purity of IgG, $F(ab')_2$ and $BsF(ab')_2$ was assessed by gel filtration on a Superdex 200 column (Pharmacia). The purity of haptens was assessed by reverse-phase HPLC chromatography. Reagent purity was greater than 90%.

The immunoreactivity of the F6 moieties, as measured in anti-F6-idiotype IgG-coated tubes (which correlates with the anti-CEA immunoreactivity), and the immunoreactivity of the 734 moiety was measured on BSA-DTPA-indium-coated tubes by incubation for 15 hr at 4°C with shaking. The anti-F6-idiotype immunoreactivities were 86%, 96% and 87% for IgG, $F(ab')_2$ and $BsF(ab')_2$, respectively. The anti-DTPA-indium immunoreactivity of the $BsF(ab')_2$ was 70%. The immunoreactivity of the labeled haptens was measured on 734 IgG coated tubes by incubation for 1 hr at 20°C with shaking. Immunoreactivity was greater than 90%. Immunoreactivity of ^{111}In-DTPA-GSA measured on 734 IgG coated tubes was 92%.

Biodistribution Kinetics

Mice bearing LS174T tumors were injected intravenously in the tail vein with 50 μl (3.7×10^4 Bq) of radiolabeled hapten or antibody supplemented with the relevant amount of unlabeled material. At selected time intervals, animals were weighed, killed with ether and dissected. The radioactivity of major organs, tumor, blood and plasma were determined. Data on relative organ weights in mice were taken from Covell et al. (*13*). The results are expressed as percent of injected dose/gram of tissue (%ID/g) or percent of injected dose/milliliter (%ID/ml).

Three-Step Experiment

The experiment was designed as follows: mice were injected with 0.2 nmol ^{131}I-labeled $BsF(ab')_2$, 20 hr later with 0.2 nmol ^{111}In-labeled DTPA-GSA and 4 hr later, with 0.1 nmol ^{125}I-labeled di-DTPA-In. Distribution of the radioactivity in the respective organs was determined 3 hr later.

Pharmacokinetic Analysis

The data from the biodistribution kinetics of the blood and of the tumor (% ID/g or % ID/ml) were fitted by least square regression to a sum of exponential $a_\alpha \times 2^{(-t/t1/2\alpha)} + a_\beta \times 2^{(-t/t1/2\beta)} + a_\gamma \times 2^{(-t/t1/2\gamma)}$, a_α, a_β or a_γ being either positive, when the blood clearance or release from the tumor were considered, or negative in the case of uptake by the tumor. For the blood, the sum of the pre-exponential coefficients was set equal to the % ID/ml at zero time calculated from the average mouse blood volume in the experiment, whereas for the tumor, the sum of the pre-exponential coefficients was set equal to 0.

The distribution volume (ml) was calculated as $1/(a\beta + a\gamma)$. The area under the time-activity curve (AUC), expressed as % ID/g $\times$ h or % ID/ml $\times$ h, was calculated by integrating the fitted exponentials from 0 to infinite time, unless otherwise indicated. Values in the text ($t_{1/2}\alpha$, $t_{1/2}\beta$, $t_{1/2}\gamma$, $a\alpha$, $a\beta$, $a\gamma$ or AUC) are given as the mean $\pm$ s.d.

Dosimetry

The activity in tumor, blood and other tissues was calculated for an injection of 100% ^{131}I-labeled material by extrapolation from the measured % ID/ml or % ID/g. AUC (Bq $\times$ s/g) were calculated by integrating the fitted exponentials out to infinite time after correction for the radioactive decay of the isotope. Tissue-absorbed beta-radiation was then calculated according to Johns et al. (*14*), using the following formula: $D\beta$ (Gy) = [1.602 10^{-16} Gy $\times$ g/Bq $\times$ s] $\times$ Eβ $\times$ AUC (Bq $\times$ s/g), with Eβ = 0.19 MeV.

RESULTS

Biodistribution of IgG and $F(ab')_2$

Mice grafted with LS174T colon carcinoma tumors were injected in duplicate with an isotopic dilution ($3.7\ 10^4$ Bq) of ^{125}I-labeled anti-CEA IgG or $F(ab')_2$ (0.2 nmol and 1.2 nmol total protein dose, respectively). Biodistribution was determined at nine time points from 5 min to 8 days.

The IgG distributed in a small volume (5.4 ml) and cleared very slowly from the blood (Table 1 and Fig. 1). The localization of the IgG into the tumor was slow but stable ($t_{1/2}\beta > 200$ hr, Table 2 and Fig. 1) with a maximal value of 32.9% $\pm$ 16.1% ID/g at 48 hr. As a result, the tumor:blood AUC ratio, calculated over 192 hr ($AUC_{0\text{-}192\ hr}$), was moderate (Table 2). The $F(ab')_2$ distributed in a similar volume (5.2 ml) but cleared more rapidly (Table 1 and Fig. 1). The localization of the $F(ab')_2$ in the tumor was more rapid and less stable (Table 2 and Fig. 1) with a peak value at 6 hr (13.2% $\pm$ 2.4% ID/g). The tumor:blood $AUC_{0\text{-}192\ hr}$ ratio was similar to IgG (Table 2). Similar results were obtained at a lower protein dose (0.2 nmol, not shown).

Optimization of Use of AES Reagents

Biodistribution of the $BsF(ab')_2$

Mice were injected with 0.2 nmol anti-CEA $\times$ anti-DTPA-In $BsF(ab')_2$, and biodistribution was determined at seven time points (from 1–48 hr). The $BsF(ab')_2$ pharmacokinetic in the blood was similar to that of $F(ab')_2$. The localization of the $BsF(ab')_2$ into the tumor was slower and less stable than that of $F(ab')_2$ but reached a higher maximum value (of 25.1% $\pm$ 0.4% ID/g after 10 hr). This is in good agreement with previously published data on modified $F(ab')_2$ fragments (*15*) and with the monovalent binding of the $BsF(ab')_2$ to the antigen. The

TABLE 1
Phamacokinetic Analysis from Blood Biodistribution Data*

Antibody (nmol)	None	$BsF(ab')_2$ 1	$BsF(ab')i2_2$ 1	$BsF(ab')_2$ 1	$F(ab')1_2$ 1,2	IgG 0.3
Delay (hr)	None	20	20	20	None	None
Hapten metal (nmol)	Bivalent indium 0.15	Bivalent indium 0.5	Bivalent yttrium 0.5	Monovalent indium 0.5	None	None
$a\alpha$ (% ID/ml)	41.8 ± 1.6†	35.7 ± 0.7	38.4 ± 1.5	38.8 ± 1.0	28.2 ± 3.9	27.8 ± 0.4
$t_{1/2}\alpha$ (min)	1.5 ± 0.3	<1‡	<1	<1	154 ± 31	153 ± 0.5
$a\beta$ (% ID/ml)	3.1 ± 1.7	6.5 ± 1.0	8.1 ± 1.5	8.5 ± 1.0	16.8 ± 3.8	18.6 ± 0.4
$t_{1/2}\beta$ (hr)	0.3 ± 0.1	11.8 ± 3.2	0.5 ± 0.1	4.2 ± 0.7	11.9 ± 1.7	163.0 ± 2.8
$a\gamma$ (% ID/ml)	0.07 ± 0.05	0.3 ± 0.9	0.04 ± 0.02	0.05 ± 0.05	0.08 ± 0.13	—
$t_{1/2}\gamma$ (hr)	8.2 ± 5.9	31.5 ± 24.7	37.5 ± 16.7	44.8 ± 31.1	>200	—
AUC (% ID/ml × hr)	3.7 ± 0.5§	125 ± 15§	8.9 ± 1.0§	55 ± 7§	403 ± 14¶	2547 ± 51¶

*Data fitted on a 0 to 8 days time scale except for the bivalent hapten alone (0 to 24 hr).
†Mean ± s.d.
‡Half-life smaller than the first experimental time.
§AUC_0
¶$AUC_{0\text{-}192\ hr}$

tumor:blood uptake ratio was 1.1 ± 0.4, 3.6 ± 0.7, and 11.1 ± 0.5 at 6, 20 and 48 hr, respectively.

Determination of Saturating $BsF(ab')_2$ Injected Dose

Mice were injected with increasing amounts of ^{125}I-labeled $BsF(ab')_2$, and biodistribution was determined 24 hr after injection (Fig. 2). The accumulation of $BsF(ab')_2$ in the tumor tended to saturate when the injected dose exceeded 5 nmol. In parallel, the tumor:blood uptake ratio decreased.

Biodistribution of Free Bivalent Hapten

After the administration of 150 pmol of ^{125}I-labeled di-DTPA-In to tumor bearing mice, the radioactivity distributed rapidly in a large volume (31.1 ml) and cleared with a $t_{1/2}\beta$ of 0.3 ± 0.1 hr (Table 1). A very small fraction circulated longer but did not correspond to any significant blood activity after 24 hr (<0.01% ID/ml). Biodistribution at 6 hr showed very low residual activities (<0.2% ID/g) in the tumor and in all tissues examined, with the exception of the kidneys (0.8% ± 0.1% ID/g). As expected, the free hapten perfused the tumor very transiently (half-lifes in minutes, Table 2).

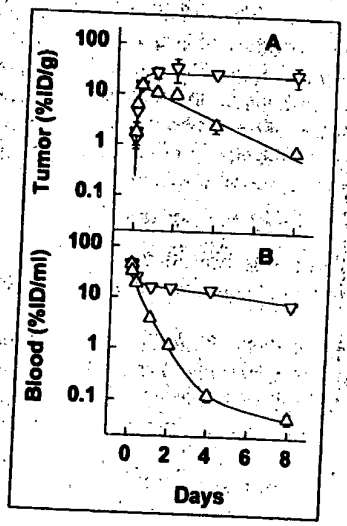

FIGURE 1. (A) Biodistribution kinetics in tumor and (B) in blood of 0.2 nmol ^{125}I-labeled F6 IgG (▽) and 1.2 nmol ^{125}I-labeled F6 $F(ab')_2$ (△). Mean ± s.d. Solid lines represent curves corresponding to parameters reported in Tables 1 and 2.

Saturation of Pretargeted $BsF(ab')_2$ by Increasing Doses of Bivalent Hapten

Mice were injected with a constant amount of ^{125}I-labeled $BsF(ab')_2$ and, 24 hr later, with increasing amounts of ^{111}In-bivalent hapten (Fig. 3). Under all the experimental conditions tested (see the figure legend), the amount of bivalent hapten that localized in the tumor tended to meet a plateau (Fig. 3A). This plateau was found to correspond reasonably well, especially regarding the biodistribution data at 48 hr, to the quantity of pretargeted $BsF(ab')_2$, in terms of bivalent binding sites, calculated taking into account the $BsF(ab')_2$ uptake by the tumor and its anti-DTPA-In immunoreactivity (1.9 ± 0.8, 1.3 ± 0.3 and 0.7 ± 0.2 pmol/g at 6, 24 and 48 hr, respectively). This suggests that, in the tumor, the bivalent hapten preferentially cross-links two $BsF(ab')_2$ molecules.

Conversely, the amount of bivalent hapten localized in the kidneys (Fig. 3B) increased linearly with the dose of bivalent hapten, a property typical of nonspecific uptake. Moreover, the amount of bivalent hapten exceeded the quantity of pretargeted $BsF(ab')_2$, in terms of DTPA binding sites (0.10 ± 0.02, 0.05 ± 0.01 and 0.02 ± 0.004 pmol/g at 6, 24 and 48 hr, respectively).

In the blood, the concentration of bivalent hapten (Fig. 3C) was independent of the hapten injected dose at 24 and 48 hr, but not at 6 hr. Furthermore, this concentration was significantly lower than the concentration of anti-DTPA $BsF(ab')_2$ binding sites under all the experimental conditions tested (0.35 ± 0.09, 0.16 ± 0.03 and 0.04 ± 0.02 pmol/g at 6, 24 and 48 hr, respectively), suggesting that the bivalent hapten did not saturate the circulating $BsF(ab')_2$ at the steady state.

Increasing Pretargeting Time

Mice were injected with 0.2 nmol $BsF(ab')_2$ and, after a variable delay (6, 20 and 48 hr), with 0.1 nmol bivalent hapten. The biodistribution was determined 24 hr later. Increasing the pretargeting time reduced the uptake of the bivalent hapten in all organs dissected. However, the uptake ratios for all organs except the kidneys increased (Fig. 4).

Decreasing Hapten Affinity

Di-In-DTPA has a high affinity for the anti-DTPA antibody ($Ka = 3.1 \pm 0.6\ nM^{-1}$) that depends on the presence of the indium ion inside the chelate. A lower affinity hapten (Ka =

TABLE 2
Phamacokinetic Analysis from Tumor Biodistribution Data*

Antibody (nmol)	None	$BsF(ab')_2$ 1	$BsF(ab')_2$ 1	$BsF(ab')_2$ 1	$F(ab')_2$ 1.2	IgG 0.3
Delay (hr)	None	20	20	20	None	None
Hapten metal (nmol)	Bivalent indium 0.15	Bivalent indium 0.5	Bivalent yttrium 0.5	Monovalent indium 0.5	None	None
Rapid $a\alpha$ (% ID/g)	5.7 ± 4.6†	8.1 ± 1.1	6.9 ± 1.4	13.3 ± 3.0	—	—
Uptake $t_{1/2}\alpha$ (min)	4.1 ± 2.2‡	4.0 ± 1.0	2.1 ± 0.9	12.4 ± 5.7	—	—
Slow $a\beta$ (% ID/g)	—	11.0 ± 6.7	—	—	15.1 ± 3.3	26.0 ± 6.7
Uptake $t_{1/2}\beta$ (hr)	—	10.4 ± 8.0	—	—	2.0 ± 0.8	3.9 ± 1.7
Rapid $a\beta$ (% ID/g)	5.5 ± 4.6	—	4.7 ± 1.4	12.6 ± 3.0	—	—
Release $t_{1/2}\beta$ (hr)	0.2 ± 0.1	—	3.3 ± 2.2	11.2 ± 4.4	—	—
Slow $a\gamma$ (% ID/g)	0.14 ± 0.04	19.1 ± 6.9	2.2 ± 0.7	0.7 ± 1.8	15.1 ± 3.3	26.0 ± 6.7
Release $t_{1/2}\gamma$ (hr)	9.1 ± 2.8	41.7 ± 7.3	36.6 ± 7.5	48.6 ± 52.6	41.3 ± 7.6	>200
AUC (% ID/g × hr)	2.8 ± 0.4§	983 ± 77§	140 ± 19§	251 ± 43§	821 ± 116¶	4559 ± 3927¶
Tumor/Blood AUC	0.75 ± 0.2	7.9 ± 1.1	15.7 ± 2.8	4.5 ± 1.0	2.0 ± 0.3	1.8 ± 1.5

*Data fitted on a 0 to 8 days time scale except for the bivalent hapten alone (0 to 24 hr).
†The sum of the pre-exponential coefficients was set equal to 0 at 0 time. Thus, in the calculation, the sign of the pre-exponential coefficients for the uptake was negative.
‡Mean ± s.d.
§AUC_0
¶$AUC_{0\text{-}192\ hr}$

2.7 ± 0.4 μM^{-1}) was obtained by saturating the DTPA group with yttrium. Mice were thus injected with 1 nmol $BsF(ab')_2$ and 20 hr later, with 0.5 nmol of either di-DTPA-Y, di-DTPA-In or mono-DTPA-In hapten (as a control high-affinity monovalent hapten, Ka of 3.6 ± 0.8 nM^{-1}).

In the blood (Table 1 and Fig. 5), di-DTPA-Y distributed in a similar volume as di-DTPA-In, but cleared 23 times faster, as expected from its lower affinity for the $BsF(ab')_2$. Interestingly, the high-affinity monovalent DTPA-In cleared three times faster. Only a very small fraction (0.3%–0.04% ID/ml) cleared very slowly. The $AUC_{0\text{-}\infty}$ for the blood was reduced about 14 and 2 times, for di-DTPA-Y and mono-DTPA-In, respectively, as compared with di-DTPA-In.

In the tumor (Table 2 and Fig. 5), the localization of di-DTPA-Y when compared with di-DTPA-In was only transient, although significant when compared to that of the free hapten. Mono-DTPA-In localization had an intermediate stability. The $AUC_{0\text{-}\infty}$ for the tumor was reduced about seven and four times, respectively, as compared with di-DTPA-In. As a result, the tumor:blood $AUC_{0\text{-}\infty}$ ratio was higher with di-DTPA-Y (15.7 ± 2.8) than with di-DTPA-In (7.9 ± 1.1) but lower with mono-DTPA-In (4.5 ± 1.0). Interestingly, the uptake into the tumor was monophasic for di-DTPA-Y and DTPA-In whereas it was biphasic for di-DTPA-In. We interpret the rapid phase as the direct uptake of the free hapten by pretargeted $BsF(ab')_2$ and the second phase as the transport of circulating hapten/$BsF(ab')_2$ complexes to the tumor.

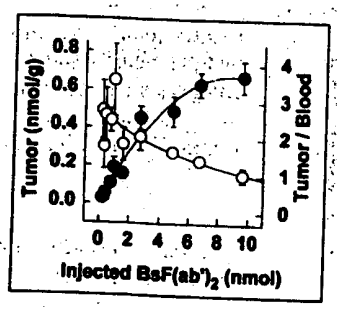

FIGURE 2. Tumor localization (—●—) and tumor:blood uptake ratio (- - -) 24 hr after administration of increasing amounts of ^{125}I-labeled $BsF(ab')_2$. Mean ± s.d.

Chase Experiments

To clear the circulating $BsF(ab')_2$ before the injection of the hapten, we used human serum albumin substituted with both DTPA and galactose (DTPA-GSA). In vitro, indium-DTPA-GSA (Ka = 3 10^7 M^{-1} for anti-DTPA-indium Fab) was able to complex the $BsF(ab')_2$ as assessed by gel filtration analysis and, in vivo, it was found to redirect circulating $BsF(ab')_2$ into the liver in a dose-dependent manner (data not shown).

In the three-step experiment, ^{111}In-labeled DTPA-GSA ac-

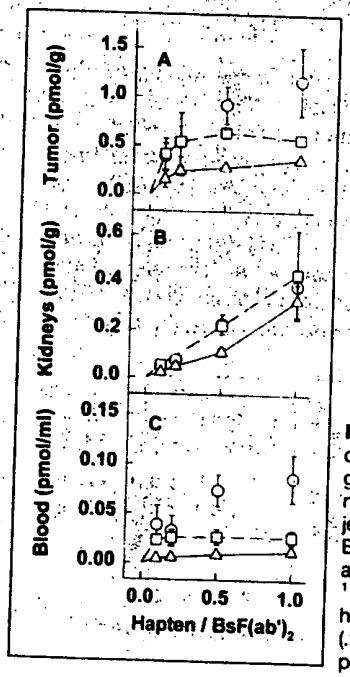

FIGURE 3. Localization of increasing doses of bivalent hapten to pretargeted $BsF(ab')_2$ (A) in tumor, (B) kidneys and (C) blood. Mice were injected with 26 pmol ^{125}I-labeled $BsF(ab')_2$ and 24 hr later with various amounts (2.6, 5.2, 13 and 26 pmol) of ^{111}In-labeled di-DTPA-In. Bivalent hapten localizations are shown at 6 (..○..), 24 (—□—) and 48 hr (—△—) posthapten injection.

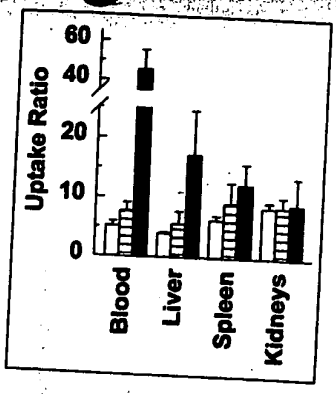

FIGURE 4. Variation of pretargeting time. Mice were injected with 0.2 nmol BsF(ab')$_2$ and after either 6 hr (▭), 24 hr (▤) or 48 hr (■) with 0.1 nmol ^{125}I-labeled di-DTPA-In. Organ distribution was determined 24 hr after bivalent hapten administration. Mean ± s.d. In tumor, localizations were 14.4 ± 1.5, 9.0 ± 2.0 and 6.1% ± 1.5% ID/g for 6-, 20- and 48-hr pretargeting time, respectively.

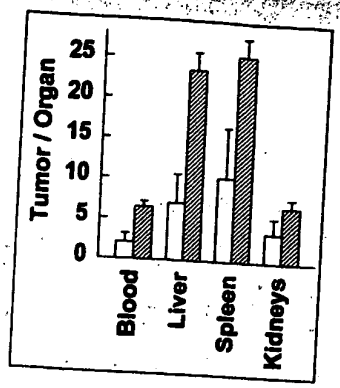

FIGURE 6. Tumor:organ uptake ratios after chase with DTPA-GSA. Mice were injected with 0.2 nmol ^{131}I-labeled BsF(ab')$_2$, 20 hr later with 0.2 nmol ^{111}In-labeled DTPA-GSA and 4 hr later with 0.1 nmol ^{125}I-labeled di-DTPA-In (▨). Control experiment was performed without clearing step (▭). Tumor: organ uptake ratios are shown at 3 hr. Mean ± s.d.

cumulated mainly in the liver (54.4% ± 13.2% ID/g). The concentration of the ^{131}I-labeled BsF(ab')$_2$ in the blood was twice as low as in the control (no chase, 6.0 ± 1.0 versus 3.3% ± 0.3% ID/ml). By contrast, its biodistribution in the tumor and major organs was not altered (data not shown). Thus, the bivalent hapten concentration was reduced twofold in the blood (2.9 ± 0.5 versus 1.4% ± 0.2% ID/ml) and in major organs but not in the tumor (5.4 ± 2.9 versus 9.3% ± 2.0% ID/g). As a consequence, tumor:organ uptake ratios were improved with the exception of the kidneys (Fig. 6).

The injection of an excess of free unlabeled hapten to clear circulating labeled hapten had been proposed earlier as a mechanism for enhancing selectivity in pretargeting experiments (*16*). Therefore, mice were injected with preformed BsF(ab')$_2$-^{125}I-labeled bivalent hapten complexes (0.1 and 0.05 nmol, respectively) and 16 hr later, with a 1–1000 times molar excess of unlabeled bivalent hapten (0.05–50 nmol, Fig. 7a) or monovalent hapten (data not shown). The monovalent and the bivalent haptens had very similar effects on the distribution of the labeled hapten in the blood and in the tumor. All the blood-borne activity could be chased in a dose-dependent way; up to 60% of the activity was chased from the tumor using a very large excess of unlabeled hapten. As expected, the injection of unlabeled hapten did not reverse the uptake of the labeled bivalent hapten in the kidneys and in catabolizing organs such as the liver (Fig. 7A).

As the injection of a 1000-fold excess of free hapten cleared more activity from the blood than from the tumor, the biodistribution kinetic was monitored before and after the chase (Fig. 7 B and C). Without chase, the localization of preformed BsF(ab')$_2$-hapten complexes was slow (half-life 3.1 ± 2.5 hr) but very stable (release half-life ≈ 200 hr; Fig. 7B). The bivalent hapten distributed in a small volume (9.0 ml) and was cleared with a $t_{1/2\beta}$ of 10.9 ± 2.8 hr (Fig. 7C). In the blood, 95% of the bivalent hapten was chased and cleared as rapidly as the free hapten (half-life = 0.25 ± 0.04 hr, and Table 1). In the tumor, the chased hapten dissociated also as rapidly as the free hapten (half-life of 0.17 ± 0.09 hr and Table 1). The remaining fraction was released slowly with an half-life of 32.0 ± 9.0 hr (Fig. 7B). This slow phase may represent either the dissociation of highly cooperative bivalent hapten-BsF(ab')$_2$ complexes or the release of sequestered (or internalized) bivalent hapten.

This chase protocol considerably improved tumor:blood uptake ratios (10 times at 6 hr after the chase) but did not improved AUC ratios. Indeed, it had a minor effect on blood $AUC_{0-6\,hr}$ (229 vs. 290% ID/ml × hr) since the AUC in the blood was determined mainly by early time points. Conversely, it lowered the tumor $AUC_{0-6\,hr}$ twofold (306 vs. 787% ID/g × hr).

Dosimetry

Dosimetry was calculated for direct targeting with IgG and F(ab')$_2$. AES targeting with 1 nmol BsF(ab')$_2$, 20 hr pretargeting time and 0.5 nmol of di-DTPA-In (referred to as AES 1/20/0.5) and AES targeting with 5 nmol BsF(ab')$_2$, 48 hr pretargeting time and 2.5 nmol di-DTPA-In (referred to as AES

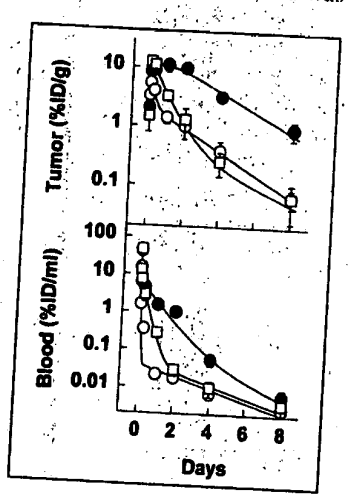

FIGURE 5. Effect of hapten affinity and valence. Mice were injected with 1 nmol BsF(ab')$_2$ and 20 hr later with either 0.5 nmol ^{125}I-labeled di-DTPA-In (—●—), di-DTPA-Y (—○—) or mono-DTPA-In hapten (—□—). Mean ± s.d. Solid lines represent curves corresponding to parameters reported in Tables 1 and 2.

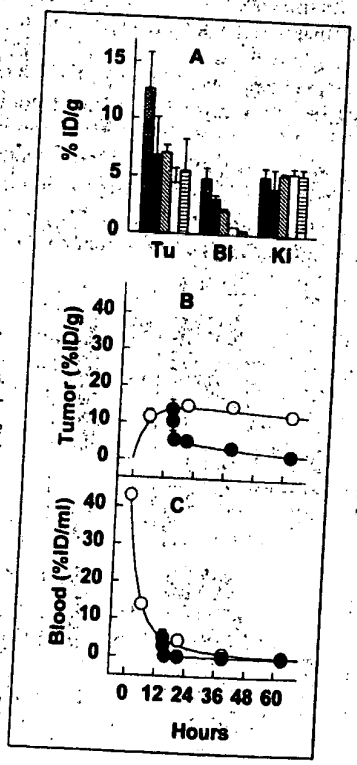

FIGURE 7. Postchase experiments. (A) Mice were injected simultaneously with 100 pmol BsF(ab')$_2$ and 50 pmol ^{125}I-labeled di-DTPA-In, and 16 hr later, with saline solution (▩) or with a 1- (■), 10- (▨), 100- (▭), or 1000-molar ( ) excess of unlabeled di-DTPA-In. Organ distribution was determined 1 hr postchase (Tu = tumor, Bl = blood, Ki = kidneys). (B, C) Tumor and blood pharmacokinetics with or without a chase step. Mice were injected as in (A) and 16 hr after, with 1000-molar excess of unlabeled di-DTPA-In (—●—) or with saline solution (—○—). Mean ± s.d.

TABLE 3
Tumor and Normal Tissue Absorbed Radiation Doses (Gy)*

	AES targeting		Direct targeting	
	AES 1/20/0.5	AES 5/48/2.5	IgG	F(ab)'2
Tumor	31.9 ± 16.4†	64.1 ± 15.9	86.2 ± 22.5	33.9 ± 6.2
Blood	4.7 ± 1.9	8.2 ± 2.8	30.1 ± 4.3	17.8 ± 3.6
Tumor/Blood	6.7 ± 4.4‡	7.8 ± 3.3	2.9 ± 0.9	1.9 ± 0.5
Tumor/Liver	10.3 ± 5.4	7.1 ± 2.2	6.8 ± 1.6	9.5 ± 2.8
Tumor/Spleen	12.1 ± 6.6	12.4 ± 5.4	4.1 ± 1.0	12.3 ± 5.1
Tumor/Kidneys	7.0 ± 3.7	4.9 ± 1.4	6.9 ± 2.6	5.9 ± 1.4

*Estimation based on an administered activity of 37 MBq ^{131}I-labeled bivalent hapten (0.5 nmol; AES 1/20/0.5), 185 MBq ^{131}I-labeled bivalent hapten (2.5 nmol, AES 5/48/2.5), 11.1 MBq ^{131}I-labeled IgG (0.2 nmol) and 44.4 MBq ^{131}I-labeled F(ab)'$_2$ (1.2 nmol).
†Absorbed radiation dose (Gy), mean ± s.d.
‡Absorbed radiation dose ratio, mean ± s.d.

5/48/2.5). For IgG and F(ab')$_2$, the activity was calculated taking into account the protein dose used in the experiment and the maximal specific activity described in the literature for antibodies labeled with ^{131}I (370 MBq/mg). As the half-life of the release of the IgG from the tumor could not be calculated, the integration on the IgG tumor data were done based solely on the physical half-life of the isotope. The di-DTPA-In hapten can be labeled with high specific activity [up to 74 MBq/nmol (*10*), Gautherot, unpublished data, 1995]. Thus, calculations were made assuming ^{131}I injected activities of 11.1 MBq for IgG, 44.4 MBq for F(ab')$_2$ which corresponds to their respective MTD (*17*) and, 37 MBq and 185 MBq for the AES protocols. Under these conditions (Table 3), the calculated cumulated doses to the tumor and tissues by direct targeting with IgG or F(ab')$_2$ were in good agreement with those reported in the literature (*18*). Similarly, both AES protocols appeared capable of delivering high radiation doses to the tumor. AES 1/20/0.5 was predicted to have an efficiency close to F(ab')$_2$ and AES 5/48/2.5 was predicted to be as efficient as IgG (Table 3).

DISCUSSION

The success of radioimmunotherapy requires high and stable tumor localization combined with low exposure of normal tissues. RAIT protocols with directly labeled antibodies are limited by the toxicity to the hematopoietic system, the bone marrow being the most radiosensitive organ. Thus, pretargeting approaches have been designed to reduce the exposure of normal tissues to radiation. However, unlike direct targeting, pretargeting strategies must be optimized carefully with respect to the doses and administration schedules (*19,20*).

The simulations performed by Baxter et al. (*21*) with a physiologically-based pharmacokinetic model suggest that the optimal dose of bispecific antibody should be just sufficient to saturate the antigen-binding sites in the tumor. Similarly, the hapten dose should be just sufficient to saturate the antibody present in the tumor, and the pretargeting time interval should be long enough to give high tumor-to-blood concentration ratios at hapten injection. In these experiments, we used the same bispecific antibody (BsF(ab')$_2$) and, in addition to the above mentioned parameters, we examined the effect of the valence and the affinity of the hapten for the BsF(ab')$_2$ on the performance of AES pretargeting for RAIT.

In the experiments presented here, particular attention was given to the BsF(ab')$_2$ to hapten molar ratio to achieve maximal uptake of bivalent hapten by the tumor while limiting the nonspecific uptake by catabolizing tissues. Provided that the BsF(ab')$_2$ dose did not exceed 5 nmol, a molar ratio of 0.5 appeared to be the best compromise.

We (*7,22*) and others (*23*) have shown the benefit of pretargeting using low doses of bispecific antibody and bivalent hapten. Similarly, therapeutic doses of bivalent hapten exhibited significantly higher targeting efficacy (high uptake and stability) and better selectivity than equivalent doses of monovalent hapten. Although at early time points, monovalent and bivalent hapten bound similarly to the BsF(ab')$_2$ in the blood and in the tumor, the final difference results from the slower release of the bivalent hapten from the tumor. Similar instability of monovalent haptens (Ka antihapten 0.1–14 nM^{-1}) has been reported in different experimental models and with other pretargeting systems (*20,24,25*). Furthermore, using a μM-affinity bivalent hapten increased the selectivity for the tumor in terms of AUC ratio but at the price of a dramatic loss of targeting efficacy. This suggests that high affinity is required for targeting efficacy, but that the selectivity ultimately relies on the affinity enhancement effect and on the distribution of the BsF(ab')$_2$ at the time of hapten injection.

The selectivity of the distribution of the modified antibody itself is of major importance. Several ways have been suggested to enhance this selectivity, including the increase of the pretargeting time and the augmentation of its affinity for the target antigen. Our data, in agreement with those of other workers (*20*), show that longer pretargeting intervals improved the selectivity but at the expense of reduced tumor localization. In this tumor model, a 10-fold increase in affinity (10^9 to 10^{10} M^{-1}) did not affect the release half-life of F(ab')$_2$ fragments from the tumor (unpublished data) suggesting that the shedding and/or the internalization, although moderate, of the CEA (*26*) may become the limiting factor.

With pretargeting strategies, the complexes between the modified antibody and the radiolabeled second component that form in the blood contribute largely to the activity in the blood. It has been shown, both experimentally (*16*) and in the clinic (*27*), that the use of an additional clearing step, in which the concentration of the modified antibody is decreased before administration of the radiolabeled species, reduces this source of activity. We introduced a chase step after the administration of the labeled bivalent hapten to reverse its binding to the BsF(ab')$_2$. This approach is of limited interest for RAIT since the AUC was reduced in the tumor and unchanged in the main organs. However, the chase protocol may be used in immunoscintigraphy since it considerably improved tumor:blood ratios at early time points. More interesting for RAIT is the elimination of the circulating BsF(ab')$_2$ before hapten injection by redirecting the antibody to the hepatic asialoglycoprotein receptor. This approach has been used succesfully in the clinic

for clearing the excess of circulating antibody-streptavidin conjugate prior ^{111}In-labeled DOTA-biotin administration (*28*). In the experiment presented here, the clearing efficiency of indium-DTPA-GSA was limited. In our view, two reasons may account for this: unlike in the above mentioned system, the concentration of BsF(ab')$_2$ in the blood at the clearing step was already low when compared to that of the streptavidin-antibody conjugate and the affinity of indium-DTPA-GSA for the BsF(ab')$_2$ is 10^8 times lower than that of biotin for avidin.

Several experimental studies in mice grafted with human colon carcinoma have shown antitumor effects with ^{131}I-labeled antibodies with estimated radiation doses to the tumor ranging from 10–90 Gy (*29*). In this study, the experimental protocols with IgG, F(ab')$_2$ and AES that were selected for dosimetry were predicted to deliver from 30–90 Gy to the tumor (Table 3).

For a similar cumulated dose, the AES pretargeting may be more efficient than direct targeting, especially with IgG, because of a more homogeneous radiation dose throughout the tumor depending on the rapid diffusion of the bivalent hapten to the center of the tumor (*19*) and on the relatively rapid diffusion of the BsF(ab')$_2$. Rapid uptake kinetics with the AES were observed also in several CEA-expressing multicell spheroids, using the same reagents (*30*).

In a recent clinical RAIT study, the dose limit to the red marrow was shown to be 4.5 Gy (*4*). In rodents, the dose limit is generally higher, 6–9 Gy (*31*). As the activity in the marrow may be considered as a fraction of the activity in the blood (*32*), we predict here that RAIT in the mouse model with AES pretargeting should be less toxic (Table 3). After the blood, the kidney, the liver and the spleen may be the dose limiting organs since AUC ratios were not improved with the AES compared to direct targeting, presumably because of prolonged intracellular retention of the activity (*33*).

The interest of AES pretargeting has been confirmed by a clinical dosimetry study in patients with medullary thyroid cancer and small-cell lung cancer (*10*). This study showed that AES pretargeting achieved high absorbed doses (11–470 Gy/MBq), especially in the case of small-sized MTC recurrences. It has been proposed that the dose scale-up from mouse to human should not be calculated from body mass ratios (≈ 2500 times) but rather as the 3/4 power of this ratio (*34*) (≈ 350 times). Thus, the 37 MBq injected to mice would correspond to 13 GBq in humans, which is an acceptable activity in terms of the medical care safety requirements. In parallel, the dose of bispecific antibody would be increased to 100–200 mg.

CONCLUSION

AES pretargeting RAIT protocols could be designed to deliver higher radiation doses to the tumor with comparable hematological toxicity as direct targeting using labeled IgG or F(ab')$_2$. Clearing agents used to reduce the concentration of circulating bispecific antibody before administration of the labeled hapten should further increase the safety of AES pretargeting.

REFERENCES

1. Press OW, Eary JF, Appelbaum FR, et al. Phase II trial of I-131-B1 (anti-CD20) antibody therapy with autologous stem cell transplantation for relapsed B cell lymphomas. *Lancet* 1995;346:336–340.
2. Kaminski MS, Zasadny KR, Francis IR, et al. Radioimmunotherapy of B-cell lymphoma with ^{131}I-anti-B1 (anti- CD20) antibody. *N Engl J Med* 1993;329:459–465.
3. Juweid M, Sharkey RM, Behr T, et al. Radioimmunotherapy of medullary thyroid cancer with iodine-131-labeled anti-CEA antibodies. *J Nucl Med* 1996;37:905–911.
4. Behr TM, Sharkey RM, Juweid ME, et al. Phase I/II clinical radioimmunotherapy with an iodine-131-labeled anti-carcinoembryonic antigen murine monoclonal antibody IgG. *J Nucl Med* 1997;38:858–870.
5. Rosebrough SF. Two-step immunological approaches for imaging and therapy. *Quarterly J Nucl Med* 1996;40:234–251.
6. Le Doussal JM, Martin M, Gautherot E, Delaage M, Barbet J. In vitro and in vivo targeting of radiolabeled monovalent and divalent haptens with dual specificity monoclonal antibody conjugates: enhanced divalent hapten affinity for cell-bound antibody conjugate. *J Nucl Med* 1989;30:1358–1366.
7. Le Doussal JM, Gruaz-Guyon A, Martin M, Gautherot E, Delaage M, Barbet J. Targeting of indium-111-labeled bivalent hapten to human melanoma mediated by bispecific monoclonal antibody conjugates: imaging of tumors hosted in nude mice. *Cancer Res* 1990;50:3445–3452.
8. Manetti C, Rouvier E, Gautherot E, Loucif E, Barbet J, Le Doussal JM. Targeting BCL$_1$ lymphoma with anti-idiotype antibodies: biodistribution kinetics of directly labeled antibodies and bispecific antibody-targeted bivalent haptens. *Int J Cancer* 1997;71:1000–1009.
9. Le Doussal JM, Chetanneau A, Guyon-Gruaz A, et al. Bispecific monoclonal antibody-mediated targeting of an indium-111-labeled DTPA dimer to primary colorectal tumors: pharmacokinetics, biodistribution, scintigraphy and immune response. *J Nucl Med* 1993;34:1662–1671.
10. Bardies M, Bardet S, Faivre-Chauvet A, et al. Dosimetric study using a bispecific antibody and a ^{131}I-labeled bivalent hapten in patients with medullary thyroid carcinoma and small-cell lung cancer. *J Nucl Med* 1996;37:1853–1859.
11. Glennie MJ, McBride HM, Worth AT, Stevenson GT. Preparation and performance of bispecific F(ab'g)$_2$ antibody containing thioether-linked Fab'g fragments. *J Immunol* 1987;139:2367–2375.
12. Janevik-Ivanoyska E, Gautherot E, Hilairet de Boisferon M, et al. Bivalent hapten peptides designed for iodine-131 pretargeted radioimmunotherapy. *Bioconjug Chem* 1997;8:526–533.
13. Covell DG, Barbet J, Holton OD, Black CD, Weinstein JN. Pharmacokinetics of monoclonal immunoglobulin G$_1$, F(ab')$_2$, and Fab' in mice. *Cancer Res* 1986;46:3669–3978.
14. Johns HE, Cunningham JR. The physics of radiology. In: Friedmann M, eds. *Monograph in the bannerstone division of American lectures in radiation therapy*. 3rd ed. Springfield, IL: Charles C. Thomas; 1978:564–574.
15. Quadri SM, Lai J, Mohammadpour H, Vriesendorp HM, Williams JR. Assessment of radiolabeled stabilized F(ab')$_2$ fragments of monoclonal antiferritin in nude mouse model. *J Nucl Med* 1993;34:2152–2159.
16. Goodwin DA, Meares CF, David GF, et al. Monoclonal antibodies as reversible equilibrium carriers of radiopharmaceuticals. *Nucl Med Biol* 1986;13:383–391.
17. Blumenthal RD, Sharkey RM, Haywood L, et al. Targeted therapy of athymic mice bearing GW-39 human colonic cancer micrometastases with ^{131}I-labeled monoclonal antibodies. *Cancer Res* 1992;52:6036–6044.
18. Sharkey RM, Motta-Hennessy C, Pawlyk D, Siegel JF, Goldenberg DM. Biodistribution and radiation dose estimates for yttrium- and iodine-labeled monoclonal antibody IgG and fragments in nude mice bearing human colonic tumor xenografts. *Cancer Res* 1990;50:2330–2336.
19. Sung C, Van Osdol WW. Pharmacokinetic comparison of direct antibody targeting with pretargeting protocols based on streptavidin-biotin binding. *J Nucl Med* 1995;36:867–876.
20. Santos O, Kindle Payne J, Domitrowsky JB, Berkeley C, Mackensen DG. A two step delivery system utilizing a bi-specific monoclonal antibody for radioimmunotherapy. *Antibody Immunoconj Radiopharm* 1995;8:93–109.
21. Baxter LT, Zhu H, Mackensen DG, Butler WF, Jain RK. Biodistribution of monoclonal-antibodies: scale-up from mouse to human using a physiologically based pharmacokinetic model. *Cancer Res* 1995;55:4611–4522.
22. Le Doussal JM, Gautherot E, Martin M, Barbet J, Delaage M. Enhanced in vivo targeting of an asymetric bivalent hapten to double-antigen-positive mouse B cells with monoclonal antibody conjugate cocktails. *J Immunol* 1991;146:169–175.
23. Goodwin DA, Meares CF, McTigue M, et al. Pretargetred immunoscintigraphy: effect of hapten valency on murine tumor uptake. *J Nucl Med* 1992;33:2006–2013.
24. Schumacher J, Klivenyi G, Matys R, et al. Multistep tumor targeting in nude mice using bispecific antibodies and a gallium chelate suitable for immunoscintigraphy with positron emission tomography. *Cancer Res* 1995;55:115–123.
25. Kranenborg MH, Boerman OC, Oosterwijk-Wakka JC, De Weijert MC, Corstens FH, Oosterwijk E. Two-step radio-immunotargeting of renal cell carcinoma xenografts in nude mice with anti-renal-cell-carcinoma x anti-DTPA bispecific monoclonal antibodies. *Int J Cancer* 1998;75:74–80.
26. Casalini P, Luison E, Menard S, Colnaghi MI, Paganelli G, Canevari S. Tumor pretargeting: role of avidin streptavidin on monoclonal antibody internalization. *J Nucl Med* 1997;38:1378–1381.
27. Paganelli G, Magnani P, Zito F, et al. Three-Step monoclonal antibody tumor targeting in carcinoembryonic antigen-positive patients. *Cancer Res* 1991;51:5960–5969.
28. Ratliff B, Reno J, Axworthy D, et al. Performance of antibody streptavidin pretargeting in patients: initial results. *J Nucl Med* 1995;36:225P.
29. Buchsbaum DJ, Langmuir VK, Wessels BW. Experimental radioimmunotherapy. *Med Phys* 1993;20:551–567.
30. Devys A, Thedrez P, Gautherot E, et al. Comparative targeting of human colon-carcinoma multicell spheroids using one- and two-step (bispecific antibody) techniques. *Int J Cancer* 1996;67:883–891.
31. Thames HD, Hendry JH. Radiation-induced injury to tissues. In: Thames HD, ed. *Fractionation in radiotherapy*. London: Taylor and Francis; 1987:1–21.
32. Sgouros G. Bone marrow dosimetry for radioimmunotherapy: theoretical considerations. *J Nucl Med* 1993;34:689–694.
33. Manetti C, Le Doussal JM, Rouvier E, Gruaz-Guyon A, Barbet J. Intracellular uptake and catabolism of anti-IgM antibodies and bi-specific antibody-targeted hapten by B-lymphoma cells. *Int J Cancer* 1995;63:250–256.
34. West GB, Brown JH, Enquist BJ. A general model for the origin of allometric scaling laws in biology. *Science* 1997;276:122–126.